Journal of Energy Storage 31 (2020) 101674

Contents lists available at ScienceDirect

Journal of Energy Storage

journal homepage: www.elsevier.com/locate/est

Hydrogen storage properties of magnesium borohydride infiltrated in silica aerogel using solvated and pressure methods

Miriam Rueda[a,*], Óscar Benito-Román[b], Alessandro Girella[c], Pacifico Cofrancesco[c], Chiara Milanese[c]

[a] Department of Chemical Engineering and Environmental Technology, University of Valladolid, Calle Doctor Mergelina s/n, 47011 Valladolid, Spain
[b] Department of Biotechnology and Food Science (Chemical Engineering Section), University of Burgos, Plaza Misael Bañuelos s/n, 09001 Burgos, Spain
[c] Pavia H_2 Lab, C.S.G.I & Department of Chemistry, Physical Chemistry Division, University of Pavia, Viale Taramelli 16, 27100 Pavia, Italy

ARTICLE INFO

Keywords:
Hydrogen storage
Magnesium borohydride
Alpha-phase
Silica aerogel
Confinement
Reversible

ABSTRACT

In this work, the polymorphic α-magnesium borohydride form was infiltrated by wet impregnation using tetrahydrofuran (THF) as solvent and subcritical carbon dioxide as innovative drying process. Pressure infiltration at high temperature was also tested as another promising method for confinement. After infiltration, onset decomposition temperature was reduced from 280 °C into 220 °C using high pressure infiltration and down to 100 °C using wet impregnation followed by CO_2 drying. Faster kinetics were obtained in both cases due the possible particle size reduction in the precipitation process of the complex hydride and the presence of silica, which could behave as an additive.

It is the first time that this complex borohydride is 6.1 wt% H_2 reversible performing the rehydrogenation at moderate conditions of 390 °C and 120 bar H_2 using silica as support. Different values were obtained after infiltration method due to the different intermediates that were obtained after the first dehydrogenation.

1. Introduction

In order to mitigate global warming, there is a need to reduce greenhouse gasses caused by the extensive use of fossil fuels as an energy source [1,2]. A quick response is needed, otherwise the temperature of the planet will rise above the 2 °C threshold, which is considered to increase the risk of natural disasters and health diseases [3]. Renewable energies such as sunlight, wind or biomass [4] may help to reduce global warming, however some drawbacks related to their unstable supply and storage in periods of low demand must be overcome. Some of these limitations can be solved by using hydrogen as an energy vector, in the so called ‘hydrogen economy’ or ‘hydrogen society’ [5–7]. More specifically, for mobile applications, the hydrogen storage method has to be safe and efficient in addition to accomplishing the targets set by the US Department of Energy (DoE) [8]. Among other requirements, a hydrogen storage system must provide high hydrogen content, fast kinetics of desorption and absorption at low temperature and pressure, and high purity of released hydrogen (Energy OoEEAR. Hydrogen Storage, 2018). Containment of hydrogen in a solid state medium demands a nontoxic and inexpensive material which can store hydrogen optimally in terms of weight and volume and with the minimum energy requirements to charge and discharge hydrogen [9,10]. Among different hydrogen storage alternatives, one of the most promising is chemical and complex hydrides [11], solid compounds that release H_2 during their thermal decomposition.

$Mg(BH_4)_2$ (MBH) is a promising complex hydride due to its high gravimetric capacity of 14.8 wt% and 146.5 kg/m^3, exceeding the targets established by the DoE. Moreover, it has the lowest desorption temperature (starts at 270–290 °C) compared to other borohydrides [12–16]. However, two drawbacks of this complex hydride are related to its low reversibility due to the formation of stable intermediates during decomposition and its complex reaction path [12]. The rehydrogenation is difficult due to the stable B_{12} structures which are formed after the dehydrogenation process. Moreover, MBH has the most complex crystal structures and the largest number of polymorphic phases among the other borohydrides [17]. Different strategies have been examined in order to improve on one hand the reversibility and the kinetics and on the other hand to decrease the temperature of the desorption reactions [18,19]. The addition of different additives or catalysts such as Ni, TiO_2, NbF_5 among others [20–23], the confinement in porous materials (mainly in carbon materials) [19,24] and the formation of composites are some of the proposals that have been studied so far [25]. As it has been reported by Rueda et al. [26], the encapsulation and confinement leads to high dispersion of the hydride in

---

[*] Corresponding author.
E-mail address: miriam.rueda.noriega@gmail.com (M. Rueda).

https://doi.org/10.1016/j.est.2020.101674
Received 31 March 2020; Received in revised form 9 July 2020; Accepted 10 July 2020

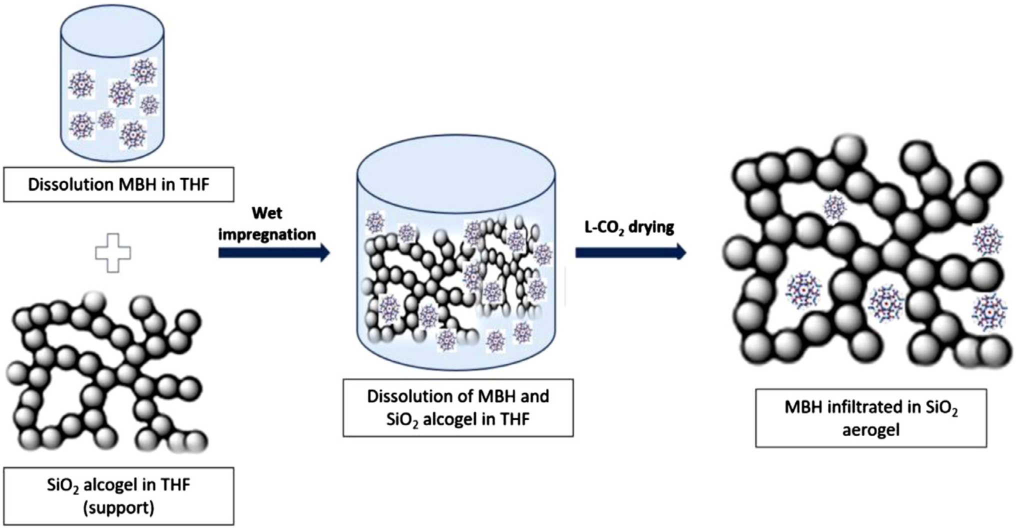

Fig. 1. Schematic process for wet impregnation followed by liquid CO_2 drying process.

the support causing the improvement of the kinetics due to the reduction of mass transfer distances. A reduction in the particle size improves both the thermodynamic properties and safety, since the access of air or moisture is hindered.

Since decomposition of $Mg(BH_4)_2$ occurs before melting, wet impregnation seems to be the most promising infiltration method. So far, only carbon hosts have been used to confine MBH by wet impregnation as method of infiltration [19] using diethyl ether [27], tetrahydrofuran (THF) [28] or ammonia [29] as solvents. In a previous work [25], composites made of commercial ϒ-$Mg(BH_4)_2$ and synthesized silica aerogel microparticles were prepared by thermal treatment in hydrogen at high pressure. After the formation of the composite with MBH, the thermal and kinetic properties of the prepared composite were improved due to the destabilization of the hydride by silica compared to bulk $Mg(BH_4)_2$. Additionally, re-hydrogenation of the prepared composite at comparatively mild conditions of 390 °C and 110 bar H_2 was done for the first time, achieving a hydrogen storage material with a reversible release of hydrogen up to 6 wt% H_2.

As the presence of silica was demonstrated to improve the properties of the complex borohydride, the present work documents the experimental trial to confine for the first time α-MBH in microparticles of silica aerogel using wet impregnation as the infiltration method. The use of an innovative process is proposed using compressed liquid carbon dioxide (CO_2) to dry the hydrogen storage material due to the promising results obtained with ammonia borane in a previous work [30]. It is the first time that α-phase is reported to be confined in a support (ϒ-MBH is known to react with CO_2 under low conditions of pressure and temperature [31]). Also, the pressure infiltration at high temperature was used in order to compare both methods of infiltration.

The prepared $Mg(BH_4)_2$–SiO_2 samples were characterized by XRPD and coupled calorimetric-manometric techniques. The kinetic curves were obtained during several hydrogen desorption-absorption cycles and compared to those of the bulk $Mg(BH_4)_2$.

2. Experimental methods

2.1. Reactants

The following substances were purchased from Sigma-Aldrich: commercial α-$Mg(BH_4)_2$ (>95% purity) and ϒ-$Mg(BH_4)_2$ (95% purity) powders, Tetramethylorthosilicate (TMOS, 98.0% purity) and ammonium hydroxide (NH_4OH, 28.0–30.0% ammonia). Methanol (MeOH; 99.8%), n-hexane (95%) and dry tetrahydrofuran (THF; with maximum water of 0.0075 wt%) were purchased from PanReac. Carburos Metálicos S.A. supplied carbon dioxide (CO_2, 99.95%).

2.2. Production of silica alcogel microparticles as support

Microparticles of silica aerogel were synthesized using a sol-gel route followed by supercritical CO_2 drying as was previously reported [30,32]. They were prepared using TMOS as precursor, methanol as solvent and hexane as dispersant in order to have small droplets of TMOS in MeOH. After 10 min of continuous mechanical stirring, an aqueous solution of NH_4OH was added as condensation catalyst, which induced the gelation of TMOS. The molar ratio used was the following: 1 mol TMOS: 4.4 mol MeOH: 3.3 mol H_2O: 4.5 mol hexane: 0.08 mol NH_4OH. These gel particles were immersed in MeOH for the aging process for at least 3 days during which the solvent was renewed 2–3 times in order to remove traces of water that had not reacted. The micro-particles of alcogel immersed in methanol were dried using supercritical CO_2 at 120 bar and 40 °C. The system was slowly pressurized and depressurized at a rate of 3 bar/min in order to avoid the cracking of the alcogel/aerogel and mechanical stresses that could damage the structural properties of the final product. Saturated CO_2 in the system was renewed four times (each drying cycle lasted 60 min, 60 min, 120 min and finally 40 min) in order to obtain completely dried particles. Dried silica aerogel microparticles had a porous structure with a surface area of 775 m^2/g and a pore volume of 3.1 cm^3/g.

2.3. Production of MBH- SiO_2 using wet impregnation and liquid CO_2 drying

A 0.6 M MBH solution was prepared dissolving 0.100 g MBH in 3 mL of THF under continuous stirring for several hours to totally dissolve the borohydride. Subsequently, micro-particles of silica alcogel aged in THF for 2 days were added to the solution to achieve a final hydrogen storage material with a ratio 1:1 MBH:SiO_2. After the addition of silica alcogel to the solution some bubbles were observed which could be hydrogen due to partial reactions of decomposition of MBH.

As a drying process, pressurized liquid CO_2 was used at 100 bar and 30 °C using the same process as previously reported in [30] (Fig. 1). As α-MBH is not reported to be soluble in CO_2, when MBH:THF-immersed alcogels are mixed with CO_2, MBH precipitates according to a GAS precipitation mechanism, thus favoring the precipitation of small particles within the pores of the gels. The sample was then stored in the inert glove box under nitrogen atmosphere until analyses were performed in order to avoid the decomposition.

While ϒ-MBH [31] was demonstrated to be converted into products such as formate and methoxy species by reaction with carbon dioxide, alpha-MBH is the only complex hydride which is not reported to be reactive with CO_2 [33].

Previous experiments performed using nitrogen drying at room temperature showed the difficulties to totally extract the solvent and totally decompose the complex hydride (alpha phase). Several solvents were tested (dichloromethane, methanol, diethyl-ether). THF was chosen as the most suitable solvent and least reactive in the presence of silica (alcogel or aerogel).

2.4. Production of MBH-SiO_2 using pressure infiltration method

Obtained SiO_2 aerogel particles were treated at 150 °C for 1 h in dynamic vacuum in the same equipment subsequently used for the infiltration in order to remove the water that was adsorbed in the surface and which could decompose MBH during infiltration. The total mass variation due to water loss corresponded to 5–7 wt%. The infiltration was performed following a similar procedure as previously reported for ϒ-MBH [25]. 100 mg of silica were mixed with 100 mg of α-MBH in a mortar. This mixture was introduced in a high pressure stainless steel sample holder under Argon atmosphere in the glove box to be transferred to the Sievert apparatus (PCT-Pro 2000, Setaram and Hy-Energy) which is described in detail in [25]. The sample was treated at 120 bar H_2 and 200 ºC for 3 h.

2.5. Characterization

All handling and preparation of the samples took place in a MBRAUN Unilab glove box which was continuously purified with argon to maintain oxygen and moisture values below 1 ppm.

Kinetic measurements and the reversibility study were conducted in the same Sievert type apparatus. Gas is analysed with a residual gas analyser (RGA Pro, Setaram & Hy-Energy) connected to the manometric instrument, confirming the presence of hydrogen.The dehydrogenation was performed at 400 °C and static vacuum and the rehydrogenation at 390 °C under 120 bar H_2 for 30 h. Bulk MBH and confined samples were rehydrogenated for 2 cycles.

Coupled manometric-calorimetric measurements were done by connecting the Sievert apparatus to a high-pressure differential scanning calorimeter (DSC, Sensys Setaram). The calorimeter cell was loaded with around 10–12 mg of the sample and heated to 460 ºC at a rate of 5 °C/min in static vacuum. Argon was used as carrier gas at 10 mL/min. Calisto was used as software for data acquisition and processing.

The crystallinity of the different samples was examined using an ex-situ X-ray powder diffractometer (model D5005 Bruker). The measuring conditions were CuKα radiation, $\lambda = 1.54060$ Å, 2θ angle ranging from 5° to 85° with a scan rate of 0.012°/min. A Bruker-dome was used in order to avoid the contact with air and to perform the measurements at room temperature under Argon atmosphere.

SEM images of the as-treated (not sputtered) powders were acquired in high vacuum using a Zeiss EVO-MA10-HR microscope. The powders were transferred under vacuum from the glove box in the SEM chamber in a homemade sample holder able to avoid the contact of the powders themselves with air.

3. Results and discussion

3.1. Comparative bulk α-MBH and ϒ-MBH phases

XRPD analyses (Fig. 2) corroborate that the commercial powders correspond to α-MBH (a) and ϒ-MBH (b) crystalline phases [17], with the former having a hexagonal structure with parameters cell of 10.3414 Å and 37.086 Å and the latter presenting a cubic cell [34] isomorphous to a hypothetical zeolite-type polymorph of SiO_2 [35]. The structure of α-MBH corresponds to COD = 2,102,921 from crystallography database, and was investigated in detail in [36].

Couple calorimetric-manometric analyses shown in Fig. 3 reveal the thermal differences between the phases. The main differences are observed in the range of temperature in which ϒ-MBH is converted into β-MBH, also known as High-Temperature (HT) phase [37]. It is shown that at 162 °C ϒ-MBH is converted to ε-MBH and at 194 °C into β phase.

α-MBH, also known as Low Temperature (LT) phase is converted directly into β phase at 226.3 °C in only one step (Figure S1) in agreement with previous findings [14,38,39]. This polymorphic transition has been reported not to be reversible, indicating that α-MBH is a metastable modification [14]. The other three peaks correspond to the reactions in which hydrogen is released, similarly to the previously reported data for ϒ-MBH [25]. Under the first two peaks (308.6 °C and 359.8 °C vs. 307 °C and 361 °C in ϒ-MBH), MBH is decomposed into MgH_2, and then in the last step (383.3 °C) into Mg [13,14].

Regarding the hydrogen release kinetics and the hydrogen content, Fig. 3 shows similar trends in both phases. Small differences in the content of hydrogen can be due to some partial decomposition.

3.2. α-MBH infiltrated in SiO_2 by wet impregnation

LT phase of MBH was infiltrated in microparticles of silica aerogel using the wet impregnation method and THF as solvent. Some prior tests were done in order to evaluate the possibility of using conventional drying in nitrogen atmosphere at room temperature. In this case, the residual solvent was very high (around 40 wt% according to the weight lost during coupled measurements) and very difficult to extract. This could be due to the formation of a MHF-THF complex [40], which, in contact with water or hydroxyl-silica groups, reacts and decomposes, even at room temperature, as reported by Solovev et al. [41]. Many bubbles were observed after the addition of silica to the solution in which MBH had been previously dissolved. This fact could be associated to the release of hydrogen and would corroborate the formation of the complex MBH-THF, recently reported Dimitrievska et al. [42] or also the possibility of reaction of MBH with the hydroxyl groups of silica. Moreover, this process could destroy the porous structure of silica aerogel due to the capillary stresses which could cause shrinkage and pore cracking [43].

Although the decomposition of α-MBH by reaction with CO_2 has not been reported so far, Fig. 4 shows that some reactions took place and part of MBH was decomposed when the experimental pressure and temperature were above the drying the conditions (100 bar, 30 °C). Only less than 2 wt% H_2 was still present in the final confined sample. This means that less than 32% of H_2 remained infiltrated after drying process which corresponds to 16 wt% MBH infiltrated rather than 50 wt %. This could be explained by the acidification of the medium due to the presence of CO_2 under subcritical conditions.

DSC analyses show the broad peak which is typical of infiltrated samples due to the higher degree of disorder created by the intimate contact with the scaffold. XRPD analyses also corroborated the infiltration giving an amorphous pattern, as it is shown in Fig. 6d.

It was observed in coupled measurements that after confinement, MBH began to release hydrogen from 100 °C, dramatically reducing the decomposition temperature. Similar results were obtained in the case of ϒ-MBH infiltrated in carbon supports obtaining onset decomposition temperature at 155 °C [19] or 100 °C [24] or even at lower temperature (75 °C) due to a synergistic effect between confinement and the addition of Nickel as catalyst [19].

3.3. MBH infiltrated in silica aerogel by high pressure treatment

Pressure infiltration was performed using the procedure reported in a previous work [25] in order to compare the wet impregnation method with an unsolvated one. When compared bulk α-MBH and α-MBH infiltrated in silica using pressure at high temperature, it was observed that the release of H_2 started at a temperature 60 °C lower (Fig. 5).

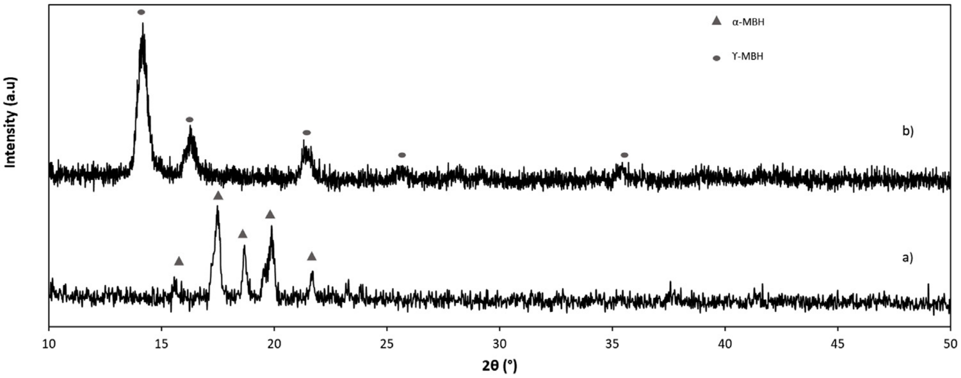

Fig. 2. XRPD profiles for commercial α-MBH (a) and ϒ-MBH (b) phases from Sigma-Aldrich.

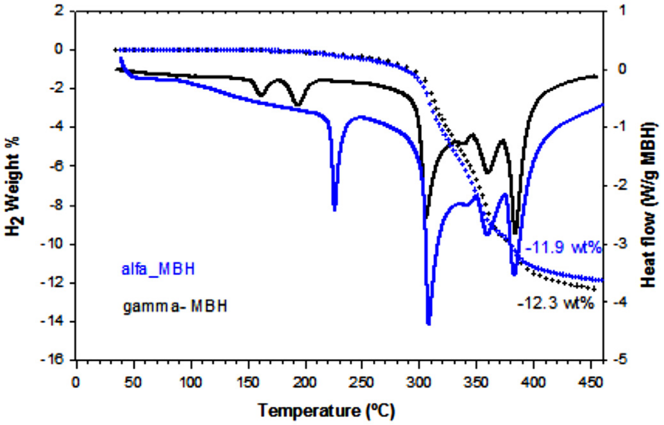

Fig. 3. Comparison of commercial bulk α-MBH and ϒ-MBH, both from Sigma Aldrich.

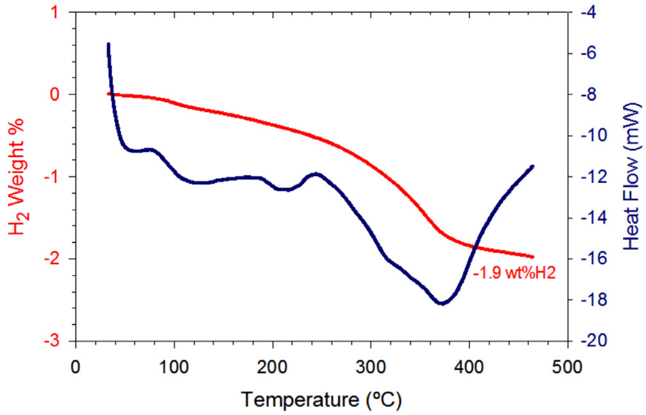

Fig. 4. Coupled calorimetric-manometric measurements of α-MBH infiltrated by wet impregnation followed by liquid CO_2 drying.

Similar results were observed with ϒ-MBH. The first peak, which corresponds to the transition from LT to HT-MBH, did not change during the infiltration treatment. Also, with this phase, three decomposition steps for bulk MBH were converted into only one broad endothermic peak and a shoulder at higher temperature in case of the prepared MBH-SiO_2 composite. This is a typical behavior of confined hydrides and is related to the intimate contact between silica and MBH.

The comparison between alfa and gamma MBH infiltrated in silica (Figure S2) provided similar results. The kinetic shape was very similar with a small difference in the final content of H_2 released (6.1 wt% H_2 vs. 6.7 wt% H_2). The dehydrogenation temperature was identical. However, in the case of ϒ-MBH, the complex borohydride was converted into β phase during pressure infiltration, whereas in this work using LT-MBH as starting material, as this change of phase takes place at higher temperature, some borohydride remained as α phase after the treatment. It was observed that the phase change (from α to β-MBH) took place at lower temperature than bulk LT-MBH after pressure treatment at high temperature.

Fig. 5 shows that 6.1 wt% H_2 was released which was more than two times the bulk MBH content (11.9 wt% H_2). This small difference could be due to instrumental error in the preparation of the mixture MBH-SiO_2 or surface oxidation of bulk MBH before the measurement. It is possible that this was due to an effect of the SiO_2 matrix as documented in a previous work [25]. This may indicate that silica could make MBH to release more hydrogen.

α-MBH remains crystalline with the same cell parameters after pressure infiltration, whereas ϒ-MBH is amorphous after the formation of the composite with silica aerogel due to the total change phase into β-MBH. LT-phase infiltrated in silica aerogel was converted into an amorphous state after the 2nd desorption.

SEM analyses (Fig. 7) corroborated the previous results. A similar morphology of the composite was observed after one desorption, which means that silica coating prevented the aggregation of particles of MBH using both methods of confinement. When comparing both methods of impregnation, it seems that in wet impregnation, the confinement is more efficient than with pressure infiltration, as crystalline particles of MBH seem to be present after pressure infiltration. This is in agreement with the XRPD results. In contrast to these results, the powder of bulk MBH was sintered into bigger agglomerates after two desorption runs. Moreover, different geometries of particles were observed in bulk MBH (some small cylinders were observed) which could correspond to different intermediates obtained comparing bulk MBH and confined samples after desorption of H_2.

3.4. Reversibility

Two cycles were performed in order to study the reversibility. The rehydrogenation was performed at 390 °C and 120 bar H_2 for 30 h. Fig. 8 shows the hydrogen release kinetics for the first and second desorption at 400 °C and vacuum of bulk MBH and MBH confined in silica aerogels by different methods reported in this work.

Bulk α-MBH showed 50.0% reversibility, which corresponds to 6.1 wt% H_2 after one cycle whereas ϒ-MH only re-hydrogenated at a 42.0% extent [25]. This is the first time that such a high reversibility has been obtained using mild conditions of pressure and temperature using this complex hydride. Compared to previous works in which ϒ phase was used, only 2.5 wt% H_2 was rehydrogenated at the same pressure used in this work and at 280 °C for 14 h [44] or even for longer times (48 h) [45]. Similar values of reversibility were obtained after rehydrogenation at harsh conditions (400 bar H_2, 270 °C for 48 h) through the formation of the stable $MgB_{12}H_{12}$ intermediate [46,47].

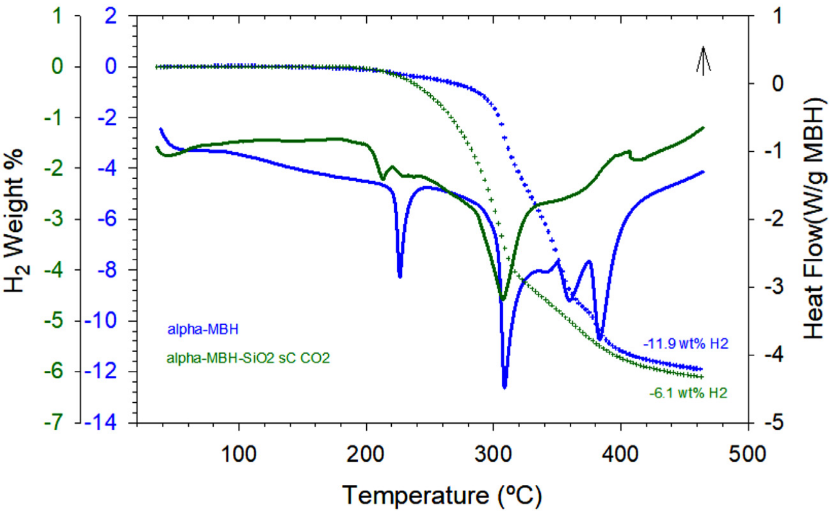

Fig. 5. Comparison between the coupled-manometric measurements of as received α-MBH vs. α-MBH infiltrated in silica aerogel by high pressure treatment.

Recently, 4.13 wt% for the second cycle and 3.24 wt% through the sixth cycle were rehydrogenated at 100 bar H_2 and 300 °C confining 40 wt% nanoparticles of ϒ-MBH in graphene [48]. It was suggested that the formation of intermediates less stable than in the case of dehydrogenation of ϒ-MBH took place and that they facilitate the rehydrogenation at milder conditions.

In the case of infiltrated samples, better results were obtained using wet impregnation and dried with liquid CO_2 compared to the pressure infiltration method. These results could be due to the precipitation of the complex hydride with lower particle size using the innovative drying method used in this work, as 53% H_2 was reversible. However, using pressure treatment, only 32.8% hydrogen was reversibly exchanged. This could be explained by the different phases observed before the first desorption. In the case of the high pressure infiltration, it was observed in coupled measurements that some α-MBH was still present, being the rest of MBH present as β phase. Because of this, a crystalline sample was obtained. However, when wet impregnation was used, since an amorphous sample was obtained and decomposition started at low temperature (100 °C), it was not possible to confirm whether it was α or β phase (this change of phase occurs at higher temperature than onset decomposition temperature). It is thought that MBH is in α state since no thermal treatment was performed before the dehydrogenation.

The problem of the solvated impregnation method using microparticles of silica aerogel as support is the low amount of MBH present after drying, due to the partial decomposition during wet impregnation and during drying with pressurized CO_2.

When silica was infiltrated in ϒ-MH by pressure infiltration [25], 42.0% H_2 was exchanged reversibly. The same value of reversibility for bulk ϒ-MBH and for composite samples was obtained, whereas in this case (using α-MBH) different behavior was observed. This difference could be explained by the different intermediates formed for bulk and infiltrated samples (in the case of α-MBH), which led to a different mechanism of decomposition over the release of H_2.

In conclusion, the order of the samples depending on the values of reversibility obtained would be the following:

1 α-MBH infiltrated by wet chemistry (WI) and liquid CO_2 drying with 53% reversibility.
2 Bulk α-MBH with 50% reversibility.

3.1. Bulk ϒ-MBH= 42%reversibility.
3.2. ϒ-MBH infiltrated by pressure infiltration (PI), also 42% reversibility.

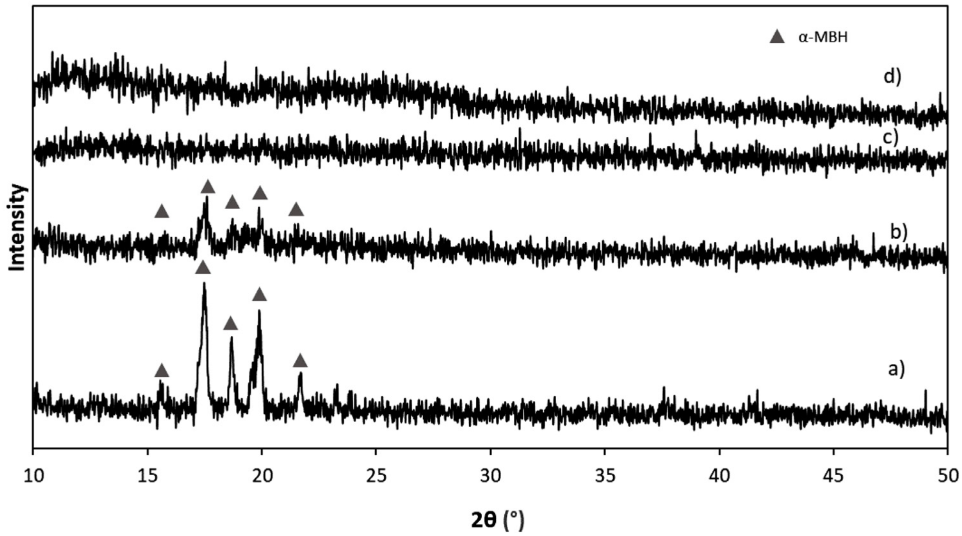

Fig. 6. XRPD patterns of bulk α-MBH a), α-MBH infiltrated in silica aerogel after pressure infiltration b) and after 2 dehydrogenation c) and α-MBH infiltrated in silica aerogel by wet chemistry and liquid CO_2 drying d).

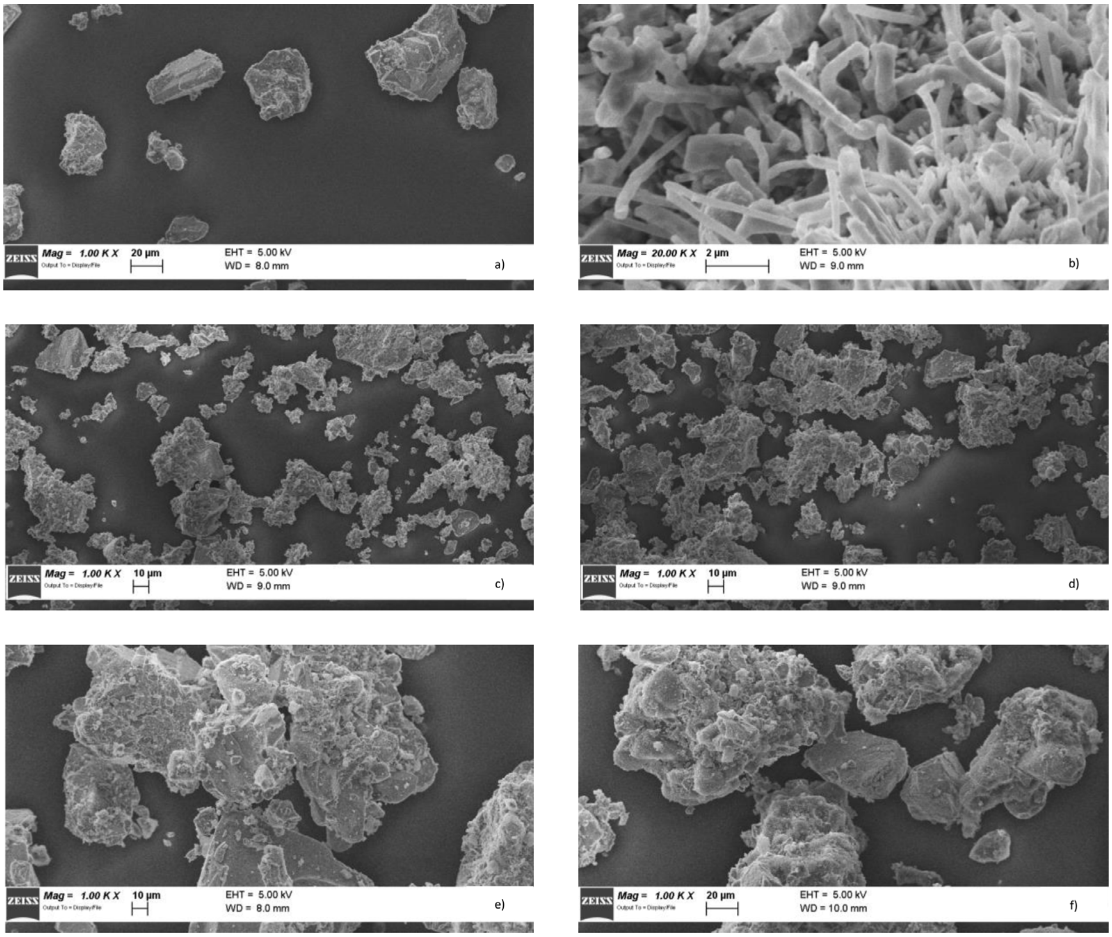

Fig. 7. SEM of a) bulk MBH and b) after 2 desorptions; c) MBH infiltrated in silica aerogel by wet impregnation and d) after desorption; e)MBH infiltrated in silica aerogel by pressure infiltrations and f) after desorption.

4 α-MBH infiltrated by pressure method with 32.8% reversibility, which can be explained by the different degree of confinement demonstrated by the crystallinity and therefore different intermediates formed after the first dehydrogenation.

The difference in reversibility and also in the rest of analyses performed can be explained by the method used to confine the complex hydride. In the case of wet impregnation followed by liquid CO_2 drying, the collapse of the pore structure is minimized or avoided altogether because carbon dioxide is miscible with the organic solvent. This fact makes the extraction happen without capillary stresses, causing the deposition of nanoparticles of MBH into the pores of the silica, which, after several cycles, leads to amorphous spectra. However, in the case of pressure infiltration, MBH is used as a technique to obtain a composite MBH-SiO_2 without assuring the confinement in the pores (crystalline MBH) and possibly producing the cracking of pores due to capillary

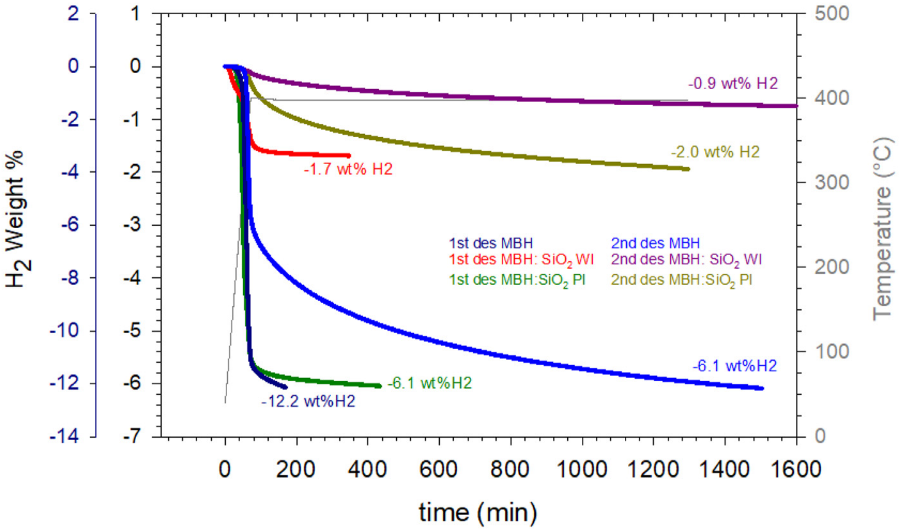

Fig. 8. Hydrogen release kinetics for the first and second desorption at 400 °C and vacuum for α-MBH (blue), α-MBH infiltrated in silica by wet impregnation followed by liquid CO_2 drying (red) and α-MBH infiltrated in silica aerogel by pressure method (green) . (For interpretation of the references to colour in this figure legend, the reader is referred to the web version of this article.)

stresses [26]. As a consequence, the benefits are associated to the presence of silica and intimal contact which is higher than simple ball-milling, whereas in the case of wet impregnation, the benefits are associated to the presence of silica and the confinement.

It was impossible to identify these intermediates both by XRPD, since amorphous patterns were obtained in all the cases after the first desorption, and by FTIR, as bonds related to MBH overlaps silica peaks [37,38].

Comparing the hydrogen release velocity in the first desorption, it is observed in Figure S3 that MBH infiltrated in silica aerogel by wet impregnation starts to release H_2 after 10 min, followed by MBH infiltrated by pressure after 30 min. Finally, bulk LT-MBH takes more time to start the dehydrogenation, after 45 min. This confirms also the results obtained in calorimetric analyses.

4. Conclusions

α-MBH was confined for the first time in silica aerogel microparticles using two different methods. Wet impregnation followed by liquid carbon dioxide drying at 100 bar and 30 °C compared to pressure infiltration at 120 bar of hydrogen and 200 °C. After confinement, the onset decomposition temperature was reduced to 100 °C and 220 °C respectively, compared to 280 °C in bulk LT-MBH. This improvement was associated to the synergistic effect between confinement and the presence of silica as support. It was also demonstrated that it was possible to rehydrogenate the composite partially at mild conditions (120 bar H_2 and 390 °C for 30 h) obtaining different values of reversibility depending on the infiltration method. 6.1 wt%H_2 was reversibly exchanged using bulk α-MBH, which is the highest value obtained so far at moderate conditions of rehydrogenation using silica as support.

Wet impregnation using THF as solvent followed by liquid CO_2 drying has been shown to be a promising method to confine hydrides. Faster kinetics and a drastic reduction of decomposition temperature was obtained. This is explained by the possible reduction of the particle size during the precipitation process of the complex hydride and the presence of silica which could behave as additive destabilizing agent. However, low amount of H_2 still remains present in the sample due to the partial decomposition during infiltration method. The search for both an adequate solvent in which the hydride is soluble and a hydride stable in CO_2 atmosphere is in progress.

Authors statement

M. Rueda: Conceptualization, Methodology, Validation, Investigation, Writing - original draft, Writing - review & editing, Project administration, Funding acquisition

O. Benito-Román: Data curation, Methodology, Writing - review & editing

A. Girella: Resources, SEM analysis, support in other analysis

P. Cofrancesco: Formal XRD analysis, review.

C. Milanese: Methodology, Project administration, Validation, Supervision

Declaration of Competing Interest

The authors declare that they have no known competing financial interests or personal relationships that could have appeared to influence the work reported in this paper.

Acknowledgements

M. Rueda thanks 'Foundation Iberdrola' for the funding in the Program 'Fellowships in Energy and Environmental Research' 2016. A. Martín is acknowledged for his support.

Supplementary materials

Supplementary material associated with this article can be found, in the online version, at doi:10.1016/j.est.2020.101674.

References

[1] C. Day, G. Day, Climate change, fossil fuel prices and depletion: the rationale for a falling export tax, Econ. Model 63 (2017) 153–160 https://doi.org/10.1016/j.econmod.2017.01.006.

[2] S. Balibar, Energy transitions after COP21 and 22, Comptes Rendus Phys. 1 (2017) 1–9 https://doi.org/10.1016/J.CRHY.2017.10.003.

[3] Z. Zoundi, CO2 emissions, renewable energy and the Environmental Kuznets Curve, a panel cointegration approach, Renew. Sustain. Energy Rev. 72 (2017) 1067–1075 https://doi.org/10.1016/j.rser.2016.10.018.

[4] F. Barbir, Transition to renewable energy systems with hydrogen as an energy carrier, Energy 34 (2009) 308–312 https://doi.org/10.1016/j.energy.2008.07.007.

[5] M. Ball, M. Weeda, The hydrogen economy - vision or reality? Int. J. Hydrogen Energy. 40 (2015) 7903–7919 https://doi.org/10.1016/j.ijhydene.2015.04.032.

[6] T. da Silva Veras, T.S. Mozer, D. da Costa Rubim Messeder dos Santos, A. da Silva César, Hydrogen: trends, production and characterization of the main process worldwide, Int. J. Hydrogen Energy 42 (2017) 2018–2033 https://doi.org/10.1016/j.ijhydene.2016.08.219.

[7] P. Tseng, J. Lee, P. Friley, A hydrogen economy: opportunities and challenges, Energy, Pergamon (2005) 2703–2720 https://doi.org/10.1016/j.energy.2004.07.015.

[8] A. Züttel, Hydrogen storage methods, (2004) 157–172. https://doi.org/10.1007/s00114-004-0516-x.

[9] D.J. Durbin, C. Malardier-Jugroot, Review of hydrogen storage techniques for on board vehicle applications, Int. J. Hydrogen Energy 38 (2013) 14595–14617 https://doi.org/10.1016/j.ijhydene.2013.07.058.

[10] G. Principi, F. Agresti, A. Maddalena, S. Lo Russo, The problem of solid state hydrogen storage, Energy 34 (2009) 2087–2091 https://doi.org/10.1016/j.energy.2008.08.027.

[11] F. Schu, B. Bogdanovic, M. Felderhoff, Light metal hydrides and complex hydrides for hydrogen storage, Chem. Commun. (Camb) 20 (2004) 2249–2258.

[12] G.L. Soloveichik, Y. Gao, J. Rijssenbeek, M. Andrus, S. Kniajanski, R.C. Bowman, S. Hwang, J. Zhao, Magnesium borohydride as a hydrogen storage material : properties and dehydrogenation pathway of unsolvated Mg (BH 4) 2, Int. J. Hydrogen Energy 34 (2009) 916–928 https://doi.org/10.1016/j.ijhydene.2008.11.016.

[13] T. Matsunaga, F. Buchter, P. Mauron, M. Bielman, Y. Nakamori, S. Orimo, N. Ohba, K. Miwa, S. Towata, A. Züttel, Hydrogen storage properties of Mg[BH4]2, J. Alloys Compd 459 (2008) 583–588 https://doi.org/10.1016/j.jallcom.2007.05.054.

[14] K. Chłopek, C. Frommen, A. Léon, O. Zabara, M. Fichtner, Synthesis and properties of magnesium tetrahydroborate, Mg(BH4)2, J. Mater. Chem. 17 (2007) 3496 https://doi.org/10.1039/b702723k.

[15] N. Hanada, K. Chłopek, C. Frommen, W. Lohstroh, M. Fichtner, Thermal decomposition of Mg(BH4)2 under He flow and H2 pressure, J. Mater. Chem. 18 (2008) 2611 https://doi.org/10.1039/b801049h.

[16] Y. Filinchuk, B. Richter, T.R. Jensen, V. Dmitriev, D. Chernyshov, H. Hagemann, Porous and dense magnesium borohydride frameworks: synthesis, stability, and reversible absorption of guest species, Angew. Chemie Int. Ed 50 (2011) 11162–11166 https://doi.org/10.1002/anie.201100675.

[17] O. Zavorotynska, A. El-kharbachi, S. Deledda, B.C. Hauback, Recent progress in magnesium borohydride Mg (BH 4) 2 : fundamentals and applications for energy storage, Int. J. Hydrogen Energy 41 (2016) 14387–14403 https://doi.org/10.1016/j.ijhydene.2016.02.015.

[18] H.-.W. Li, K. Kikuchi, Y. Nakamori, K. Miwa, S. Towata, S. Orimo, Effects of ball milling and additives on dehydriding behaviors of well-crystallized Mg(BH4)2, Scr. Mater 57 (2007) 679–682 https://doi.org/10.1016/j.scriptamat.2007.06.052.

[19] M.A. Wahab, A. Jia, D. Yang, X. Yao, Enhanced hydrogen desorption of Mg(BH4)2 by combining nanoconfinement and Ni catalyst, J. Mater. Chem. A (2013) 2–3.

[20] I. Saldan, C. Frommen, I. Llamas-Jansa, G.N. Kalantzopoulos, S. Hino, B. Arstad, R.H. Heyn, O. Zavorotynska, S. Deledda, M.H. Sørby, H. Fjellvåg, B.C. Hauback, Hydrogen storage properties of γ–Mg(BH4)2 modified by MoO3 and TiO2, Int. J. Hydrogen Energy 40 (2015) 12286–12293 https://doi.org/10.1016/j.ijhydene.2015.07.082.

[21] Z.G. Zhang, H. Wang, J.W. Liu, M. Zhu, Thermal decomposition behaviors of magnesium borohydride doped with metal fluoride additives, Thermochim. Acta 560 (2013) 82–88 https://doi.org/10.1016/j.tca.2013.02.031.

[22] A. Al-Kukhun, H.T. Hwang, A. Varma, NbF 5 additive improves hydrogen release from magnesium borohydride, Int. J. Hydrogen Energy 37 (2012) 17671–17677 https://doi.org/10.1016/j.ijhydene.2012.09.097.

[23] C. Paduani, P. Jena, Role of Ti-based catalysts in the dehydrogenation mechanism of magnesium borohydride: a cluster approach, Int. J. Hydrogen Energy 38 (2013) 2357–2362 https://doi.org/10.1016/j.ijhydene.2012.11.060.

[24] Y. Yan, Y.S. Au, D. Rentsch, A. Remhof, P.E. de Jongh, A. Züttel, Reversible hydrogen storage in Mg(BH4)2/carbon nanocomposites, J. Mater. Chem. A. 1 (2013) 11177 https://doi.org/10.1039/c3ta12222k.

[25] M. Rueda, L.M. Sanz-Moral, A. Girella, Reversible hydrogen sorption in the composite made of magnesium borohydride and silica aerogel, Int. J. Energy Res 41 (2016) 15245–15253 https://doi.org/10.1016/j.ijhydene.2016.07.074.

[26] M. Rueda, L.M. Sanz-Moral, Á. Martín, Innovative methods to enhance the

properties of solid hydrogen storage materials based on hydrides through nanoconfinement: a review, J, Supercrit. Fluids 141 (2018) 198–217 https://doi.org/10.1016/j.supflu.2018.02.010.

[27] M. Fichtner, Z. Zhao-Karger, J. Hu, A. Roth, P. Weidler, The kinetic properties of Mg (BH4)2 infiltrated in activated carbon, Nanotechnology 20 (2009) 204029https://doi.org/10.1088/0957-4484/20/20/204029.

[28] M.A. Wahab, D.J. Young, A. Karim, S. Fawzia, J.N. Beltramini, Low-temperature hydrogen desorption from Mg(BH4)2 catalysed by ultrafine Ni nanoparticles in a mesoporous carbon matrix, Int. J. Hydrogen Energy 41 (2016) 20573–20582 https://doi.org/10.1016/j.ijhydene.2016.09.098.

[29] A. Ampoumogli, T. Steriotis, P. Trikalitis, D. Giasafaki, E.G. Bardaji, M. Fichtner, G. Charalambopoulou, Nanostructured composites of mesoporous carbons and boranates as hydrogen storage materials, J. Alloys Compd 509 (2011) S705–S708 https://doi.org/10.1016/j.jallcom.2010.10.098.

[30] M. Rueda, L.M. Sanz-Moral, J.J. Segovia, Á. Martín, Improvement of the kinetics of hydrogen release from ammonia borane confined in silica aerogel, Microporous Mesoporous Mater 237 (2017) 189–200 https://doi.org/10.1016/j.micromeso.2016.09.030.

[31] J.G. Vitillo, E. Groppo, E.G. Bardají, M. Baricco, S. Bordigaa, J.G. Vitillo, E. Groppo, G. Bardají, M. Baricco, Fast carbon dioxide recycling by reaction with γ -Mg (BH 4) 2, Phys. Chem. Chem. Phys 16 (2014) 22482–22486 https://doi.org/10.1039/C4CP03300K.

[32] M. Rueda, L.M. Sanz-Moral, A. Nieto-Márquez, P. Longone, F. Mattea, Á. Martín, Production of silica aerogel microparticles loaded with ammonia borane by batch and semicontinuous supercritical drying techniques, J. Supercrit. Fluids. 92 (2014) 299–310 https://doi.org/10.1016/j.supflu.2014.06.012.

[33] T. Wartik, R.K. Pearson, Reactions of carbon dioxide with sodium and lithium borohydrides, J. Inorg. Nucl. Chem. 7 (1958) 404–411 https://doi.org/10.1016/0022-1902(58)80250-X.

[34] J. Her, W. Peter, Y. Gao, G. L.Soloveichik, J. Rijssenbeek, M. Andrus, J.-.C. Zhao, Structure of unsolvated magnesium borohydride, Acta Crystallogr 63 (2007) 561–568 B https://doi.org/10.1107/S0108768107022665.

[35] M.D. Foster, O.D. Friedrichs, R.G. Bell, F.A.A. Paz, J. Klinowski, O. Keeffe, Chemical evaluation of hypothetical uninodal zeolites, 9 (2004) 9769–9775. https://doi.org/10.1021/ja037334j.

[36] J.H. Her, P.W. Stephens, Y. Gao, G.L. Soloveichik, J. Rijssenbeek, M. Andrus, J.C. Zhao, Structure of unsolvated magnesium borohydride Mg(BH4)2, Acta Crystallogr. Sect. B Struct. Sci 63 (2007) 561–568 https://doi.org/10.1107/S0108768107022665.

[37] O. Zavorotynska, A. El-Kharbachi, S. Deledda, B.C. Hauback, Recent progress in magnesium borohydride Mg(BH4)2: fundamentals and applications for energy storage, Int. J. Hydrogen Energy (2015), https://doi.org/10.1016/j.ijhydene.2016.02.015.

[38] Y. Filinchuk, R. Cerny, H. Hagemann, Insight into Mg(BH4)2 with synchrotron X-ray diffraction: structure revision, crystal chemistry, and anomalous thermal, Chem. Mater. 21 (2009) 925–933.

[39] I. Saldan, Decomposition and formation of magnesium borohydride, Int. J. Hydrogen Energy 41 (2016) 11201–11224 https://doi.org/10.1016/j.ijhydene.2016.05.062.

[40] M. Chong, T. Autrey, C.M. Jensen, Lewis base complexes of magnesium borohydride : enhanced kinetics and product selectivity upon hydrogen release, Inorganics 5 (2017) 1–8 https://doi.org/10.3390/inorganics5040089.

[41] M.V. Solovev, O.V. Chashchikhin, P.V. Dorovatovskii, V.N. Khrustalev, A.S. Zyubin, T.S. Zyubina, O.V. Kravchenko, A.A. Zaytsev, Y.A. Dobrovolsky, Hydrolysis of Mg (BH 4) 2 and its coordination compounds as a way to obtain hydrogen, J. Power Sources 377 (2018) 93–102 https://doi.org/10.1016/j.jpowsour.2017.11.090.

[42] M. Dimitrievska, M. Chong, M.E. Bowden, H. Wu, W. Zhou, I. Nayyar, B. Ginovska, T. Gennett, T. Autrey, C.M. Jensen, T.J. Udovic, Structural and reorientational dynamics of tetrahydroborate (BH4-) and tetrahydrofuran (THF) in a Mg(BH4) 2•3THF adduct: neutron-scattering characterization, Phys. Chem. Chem. Phys 22 (2019) 368–378 https://doi.org/10.1039/c9cp03311d.

[43] A. Soleimani Dorcheh, M.H. Abbasi, Silica aerogel; synthesis, properties and characterization, J. Mater. Process. Technol 199 (2008) 10–26 https://doi.org/10.1016/j.jmatprotec.2007.10.060.

[44] O. Zavorotynska, S. Deledda, B.C. Hauback, Kinetics studies of the reversible partial decomposition reaction in Mg(BH4)2, Int. J. Hydrogen Energy 41 (2016) 9885–9892 https://doi.org/10.1016/j.ijhydene.2016.02.153.

[45] M. Chong, A. Karkamkar, T. Autrey, S. Orimo, S. Jalisatgi, C.M. Jensen, Reversible dehydrogenation of magnesium borohydride to magnesium triborane in the solid state under moderate conditions, Chem. Commun. (Camb) 47 (2011) 1330–1332 https://doi.org/10.1039/c0cc03461d.

[46] S.O.H.W. Li, K. Kikuchi, Y. Nakmori, N. Ohba, M. Miwa, S. Towata, Dehydriding and rehydriding processes of well- crystallized Mg (BH4) 2 accompanying with formation of intermediate compounds, Acta Mater 56 (2008) 1342–1347 https://doi.org/10.1016/j.actamat.2007.11.023.

[47] K.Miwa H.W.Li, N. Ohba, T. Fujita, T. Sato, Y. Yan, S. Towata, M.W. Chen, S. Orimo, Formation of an intermediate compound with a B12H12 cluster: experimental and theoretical studies on magnesium borohydride Mg(BH4)2, Nanotechnology 20 (2009) 204013https://doi.org/10.1088/0957-4484/20/20/204013.

[48] H. Zhang, G. Xia, J. Zhang, D. Sun, Z. Guo, X. Yu, Graphene-tailored thermodynamics and kinetics to fabricate metal borohydride nanoparticles with high purity and enhanced reversibility, Adv. Energy Mater (2018) 1702975–1702975 https://doi.org/10.1002/aenm.201702975.